Supporting Information

Hydrogen bonding steers the product selectivity of electrocatalytic CO reduction

Jingyi Li,[†,‡] Xiang Li,[†,‡] Charuni M. Gunathunge,[†] and Matthias M. Waegele[*,†]

†*Department of Chemistry, Merkert Chemistry Center, Boston College, Chestnut Hill, MA 02467, USA*

‡*Contributed equally to this work*

E-mail: waegele@bc.edu

List of Figures

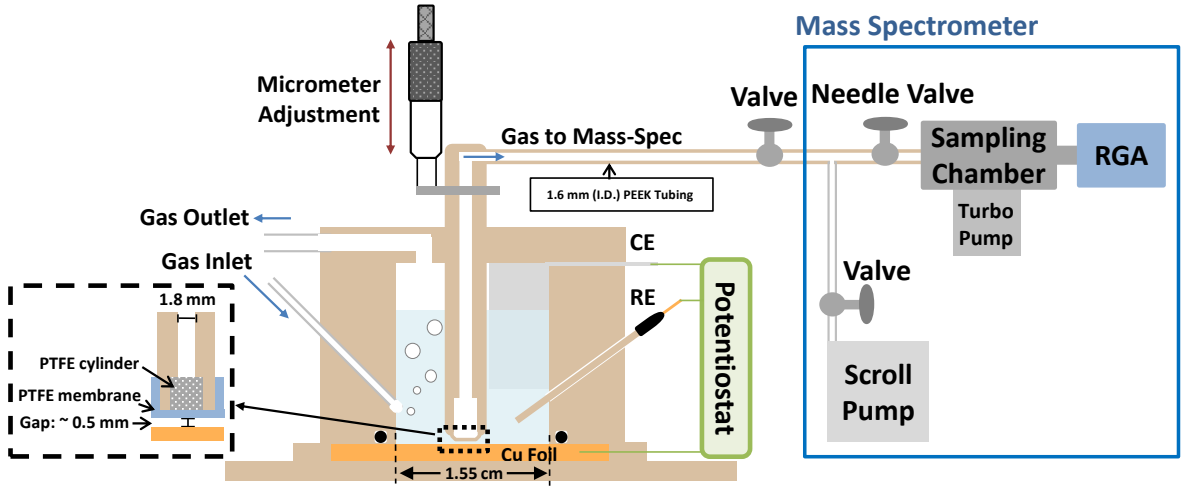

Fig. S 1: DEMS setup. A description of the setup is given in the Materials and Methods section of the main text.

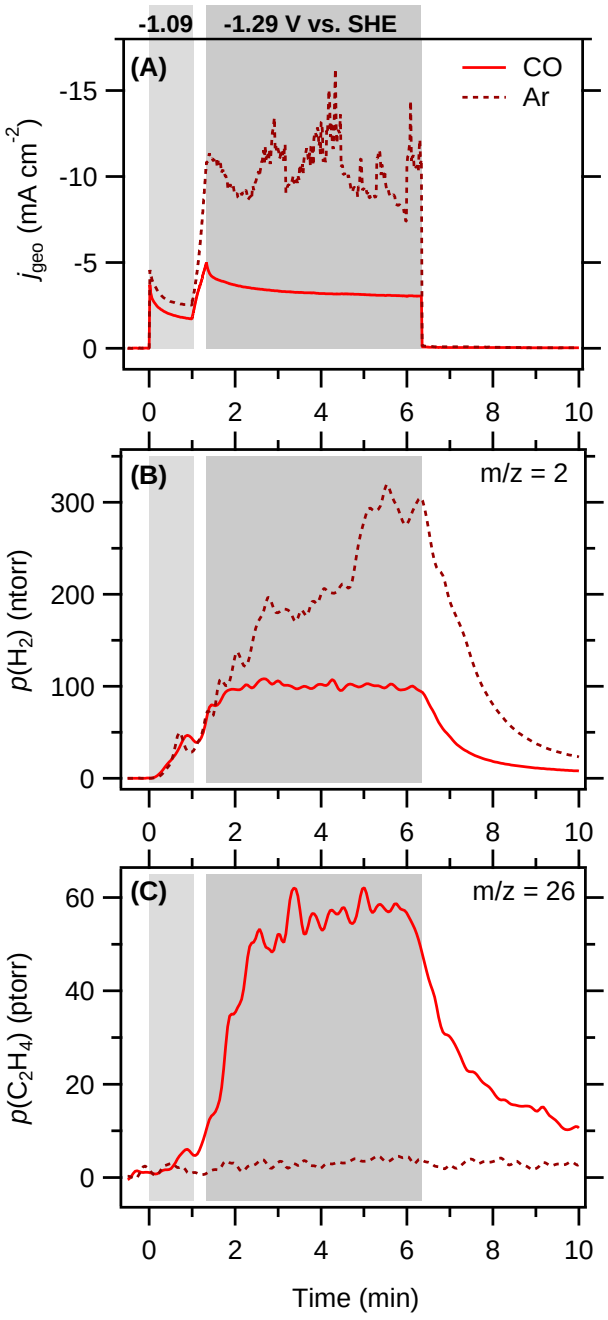

Fig. S 2: The $m/z = 26$ signal is absent in Ar-purged electrolyte. (A) Electrochemical current density during the DEMS measurements. (B) H_2 partial pressure, and (C) C_2H_4 partial pressure in the presence of aqueous solutions of 0.1 M methyl$_4$N$^+$ borate under 1 atm of CO (solid line) or Ar (dashed line). At high current densities ($\approx$ 10 mA cm^{-2}), hydrogen bubbles cover the electrode within a few seconds. Stochastic desorption of the bubbles causes the observed current density fluctuations. A significant fraction of the bubbles does not interact with the sampling tip. Therefore, a fraction of the hydrogen escapes mass spectrometric detection, giving rise to discrepancies between current density and detected hydrogen partial pressure.

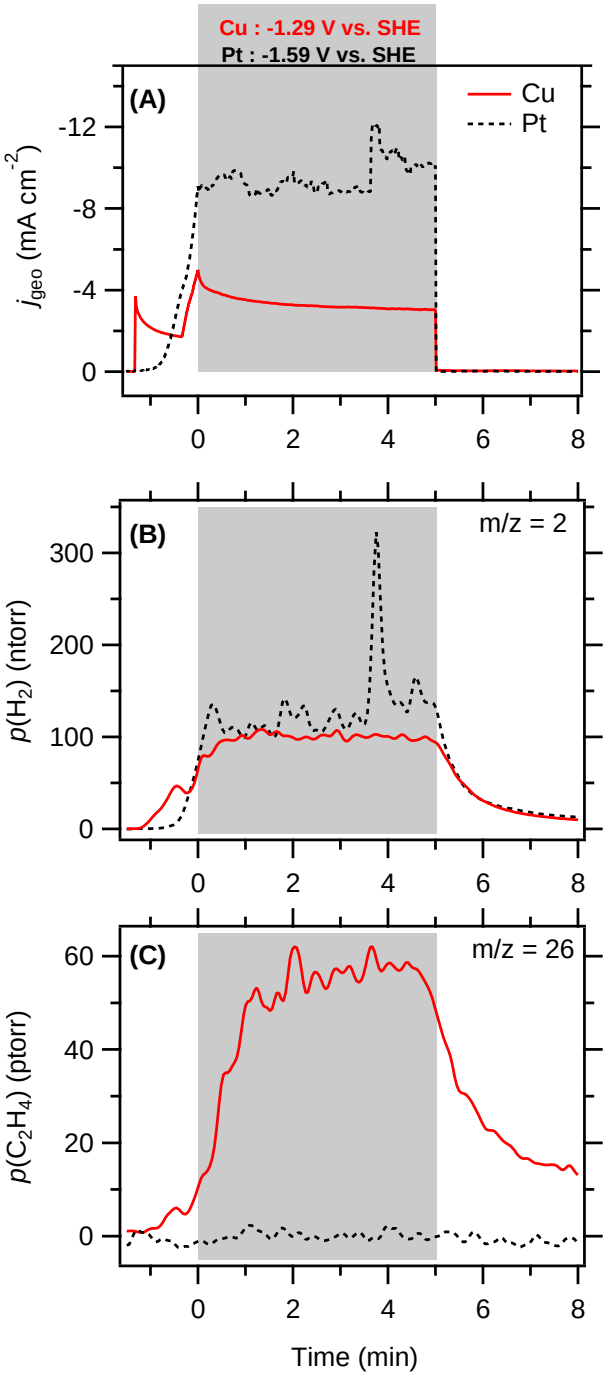

Fig. S 3: The $m/z = 26$ signal is absent when a Pt electrode is used. (A) Electrochemical current density during the DEMS measurements. (B) H_2 partial pressure, and (C) C_2H_4 partial pressure in the presence of aqueous solutions of 0.1 M methyl$_4$N$^+$ borate under 1 atm of CO on Cu (solid line) or Pt (dashed line). Reaction potentials that gave the same amount of detected H_2 were chosen. The lower H_2 detection efficiency in the case of Pt compared to the experiments with Cu is attributed to differences in H_2 bubble nucleation, potentially due to differences in surface morphology. Further, the thin Pt foil has a higher propensity to warp (compared to the thick Cu sheet electrodes). Therefore, the electrode-sampling tip distance for the experiments with Pt could not be precisely controlled. This distance impacts the collection efficiency.

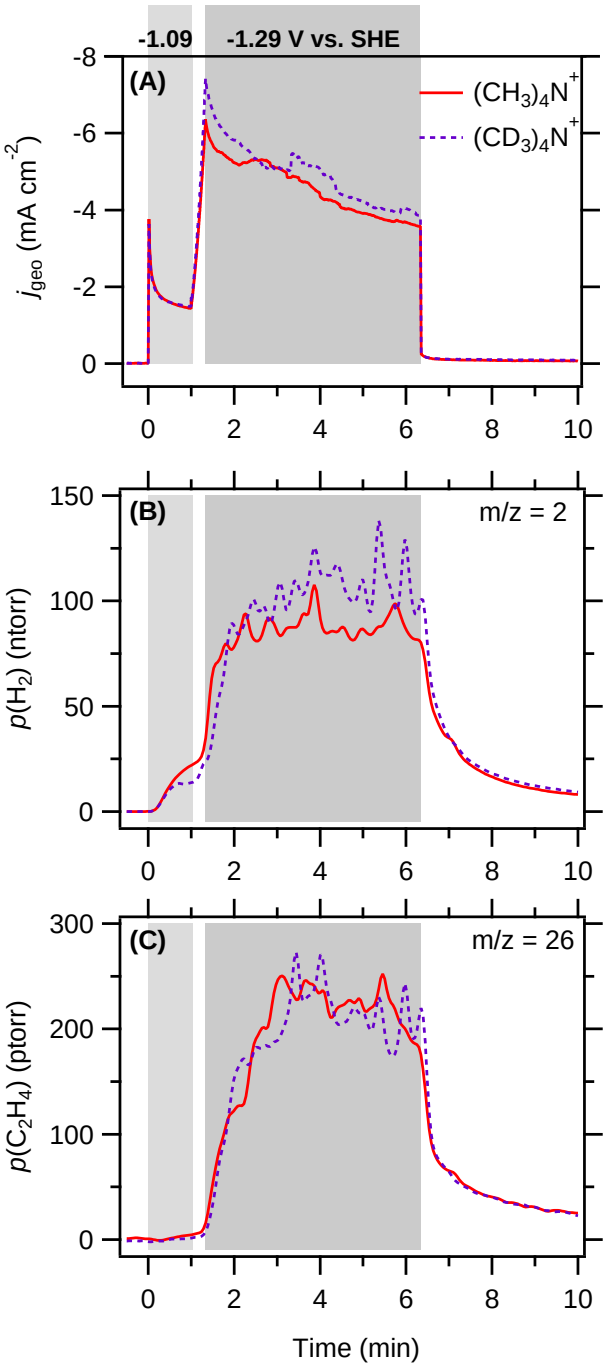

Fig. S 4: The $m/z = 26$ signal is unaffected by the use of deuterated alkyl$_4$N$^+$. (A) Electrochemical current density during the DEMS measurements. (B) H_2 partial pressure, and (C) C_2H_4 partial pressure detected in the presence of aqueous solutions of 0.1 M $(CH_3)_4N^+$ (solid line) and $(CD_3)_4N^+$ chlorides (dashed line) under 1 atm CO.

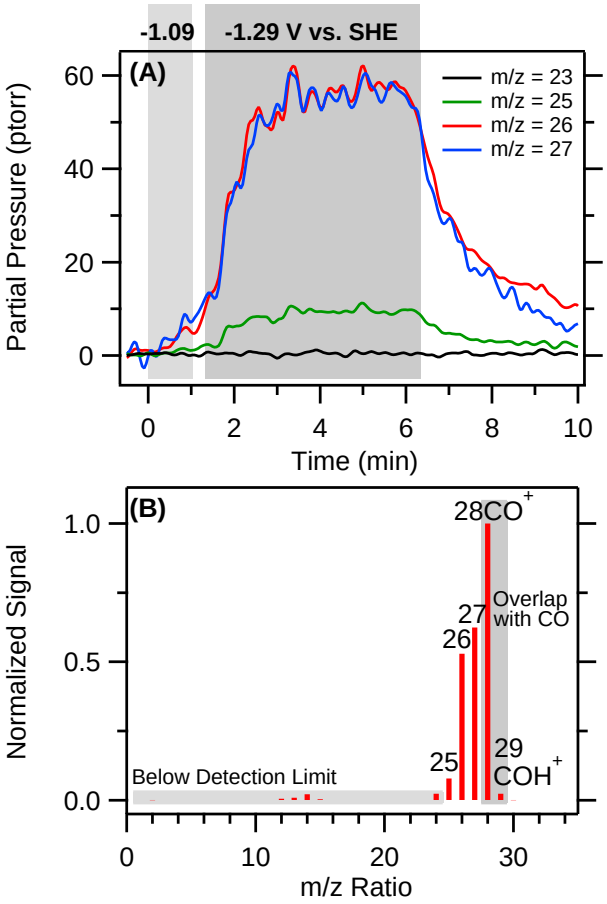

Fig. S 5: The relative partial pressures of the observable m/z values are consistent with the relative signal intensities of the standard mass spectrum of C_2H_4. (A) $m/z = 23$, 25, 26, 27 signals for the 0.1 M methyl$_4$N$^+$-experiment presented in Figure 1C of the main text. (B) Normalized standard mass spectrum of C_2H_4 from the NIST Chemistry Webbook.[1]

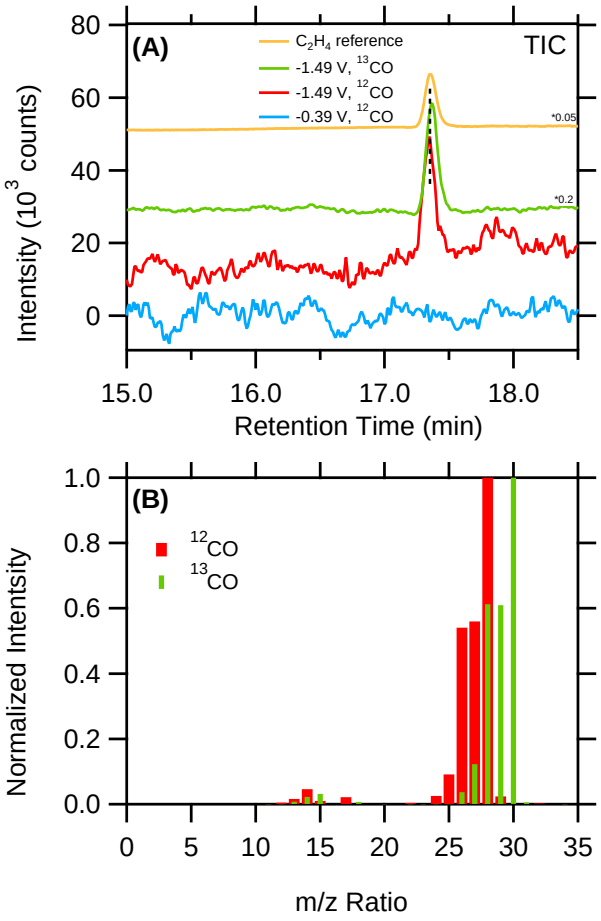

Fig. S 6: GC-MS confirms of the formation of ethylene by CO reduction. (A) GC-MS total ion chromatograms (TIC) of a C_2H_4 standard sample and gaseous products of electrolysis in CO-saturated aqueous solutions of 0.1 M methyl$_4$N$^+$ borate as indicated. (B) Mass spectra of the chromatogram peaks at 17.35 min obtained from the gaseous products collected during electrolysis at −1.49 V vs. SHE. GC-MS experiments were carried out in an H-cell. The cathode and anode compartments were separated by a Selemion AMV anion-exchange membrane (AGC Engineering Co.; Chiba, Japan). Each compartment contained 10 mL of electrolyte. Prior to the start of electrolysis, the electrolyte was saturated with CO and the cell was sealed. 100 μL of gaseous sample from the headspace of the cell was injected into GC-MS after 40 min of electrolysis.

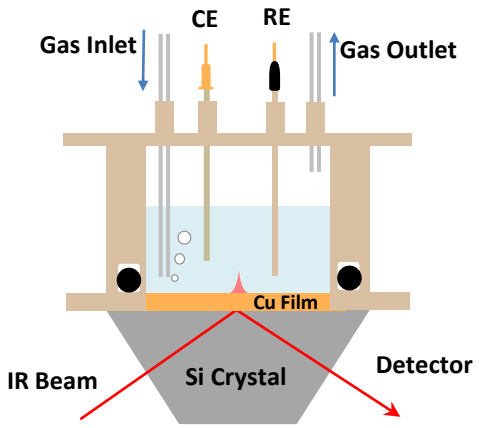

Fig. S 7: Scheme of spectroelectrochemical cell.

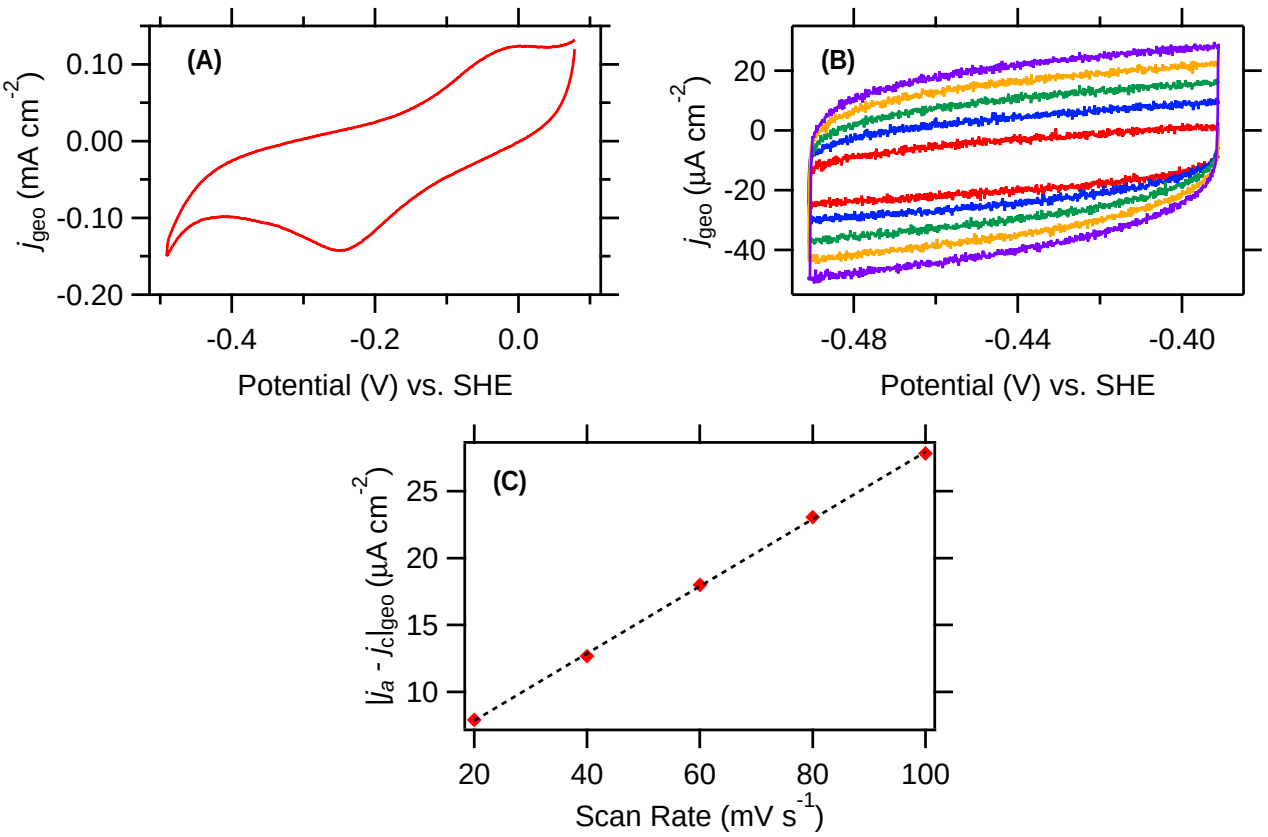

Fig. S 8: (A) Representative cyclic voltammogram obtained following five Cu film cleaning cycles from 0.08 to −0.49 V at a scan rate of 50 mV s^{-1}. (B) Representative CVs taken at scan rates of 20 (red), 40 (blue), 60 (green), 80 (yellow), and 100 mV s^{-1} (purple) to measure the double layer capacitance. (C) The double layer charging current vs. scan rate for the data shown in graph (B) (red squares) and the linear fit (black dotted line) to the data. The roughness of the film was calculated by dividing the slope of the fitted line in graph (C) by a factor of two and a reference double layer capacitance value of 28 μF cm^{-2} for a smooth Cu surface.[2]

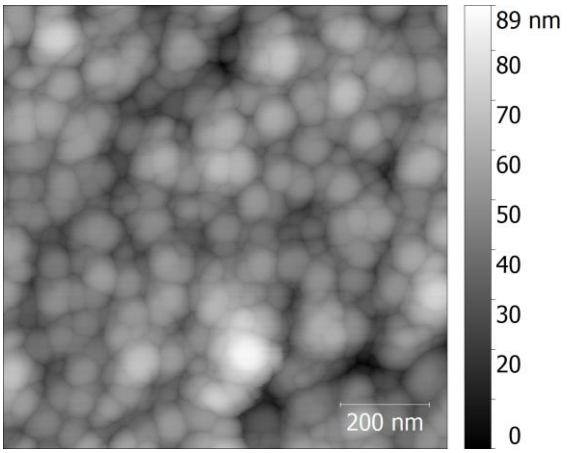

Fig. S 9: AFM image of an as-synthesized Cu film on a Si ATR crystal.

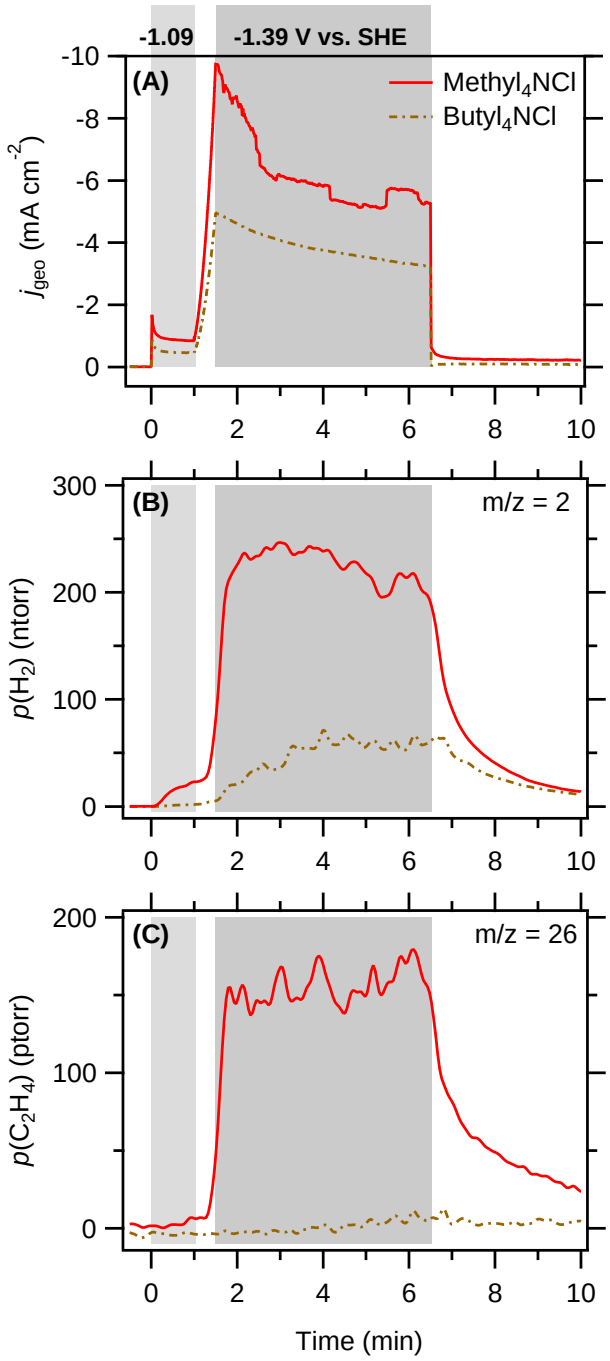

Fig. S 10: The observed trends in the $m/z = 26$ signal are also obseved in the presence of the chloride anion. (A) Electrochemical current density during the DEMS measurements. (B) H_2 partial pressure, and (C) C_2H_4 partial pressure detected in the presence of aqueous solutions of 0.1 M methyl$_4$N$^+$ chloride (solid line) and butyl$_4$N$^+$ chloride (dashed line) under 1 atm CO.

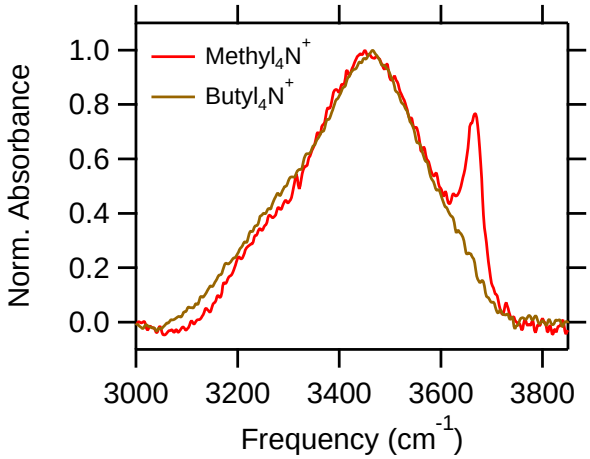

Fig. S 11: The normalized O−H stretch spectra in the presence of aqueous solutions of 0.1 M methyl$_4$N$^+$ and butyl$_4$N$^+$ borate at −1.29 V. The 3675 cm^{-1} band is prominent in methyl$_4$N$^+$-containing electrolyte but absent in the presence of butyl$_4$N$^+$.

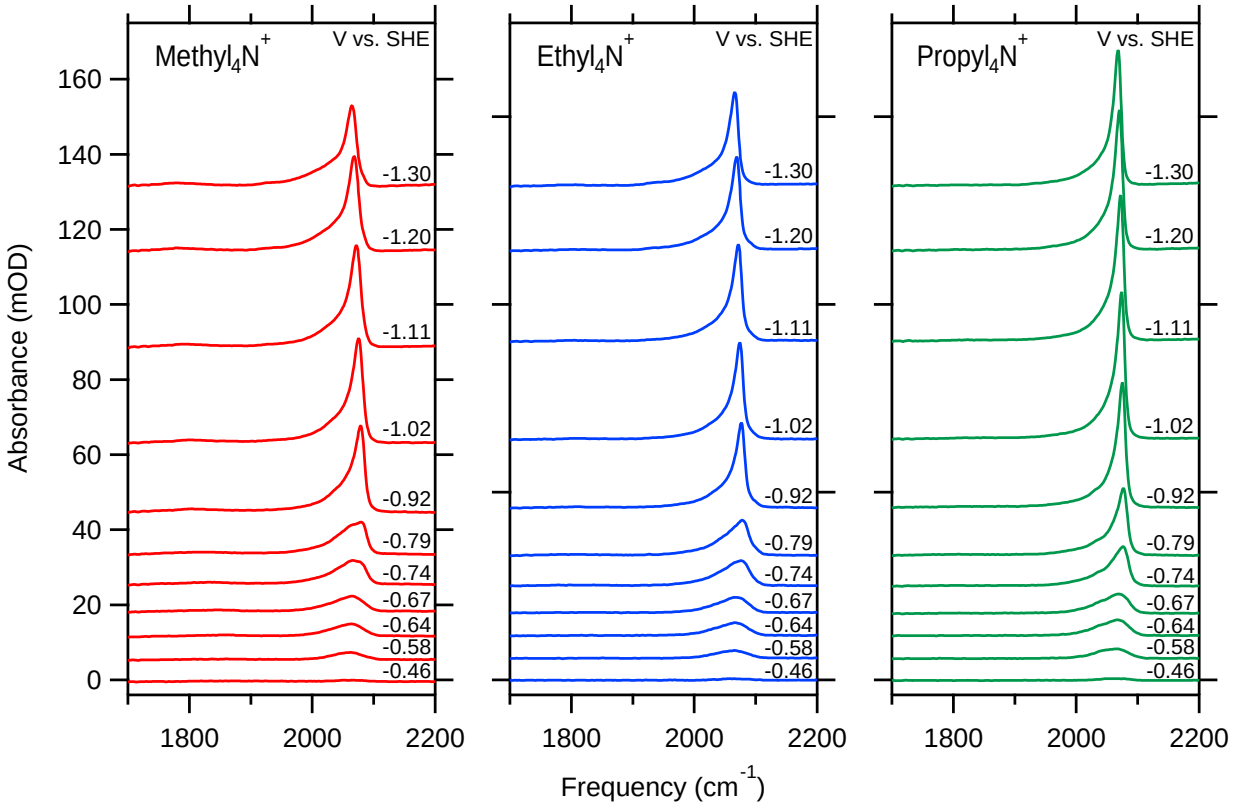

Fig. S 12: Representative CO stretch spectra in solutions of 0.1 M methyl$_4$N$^+$, ethyl$_4$N$^+$, and propyl$_4$N$^+$ chloride in D_2O.

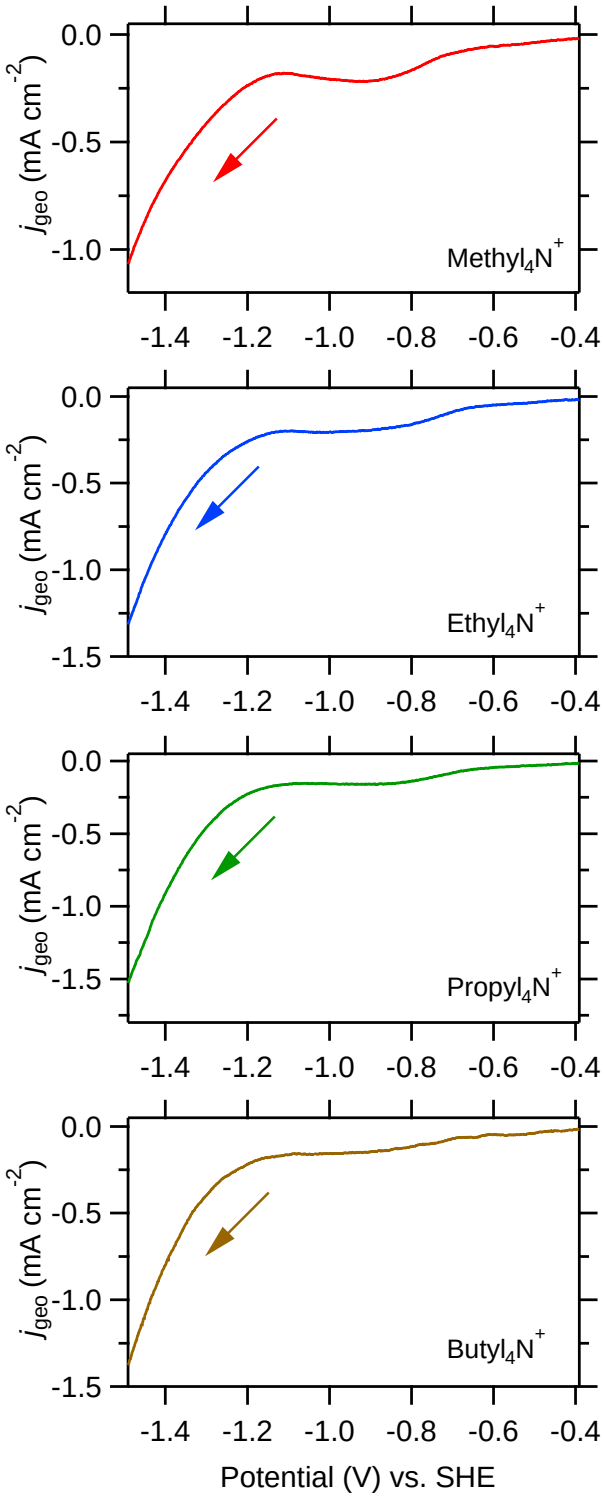

Fig. S 13: Linear sweep voltammetry current-voltage curves for the spectroscopic data presented in the main text (Figure 2) and Fig. S12. Arrows indicate the sweep direction.

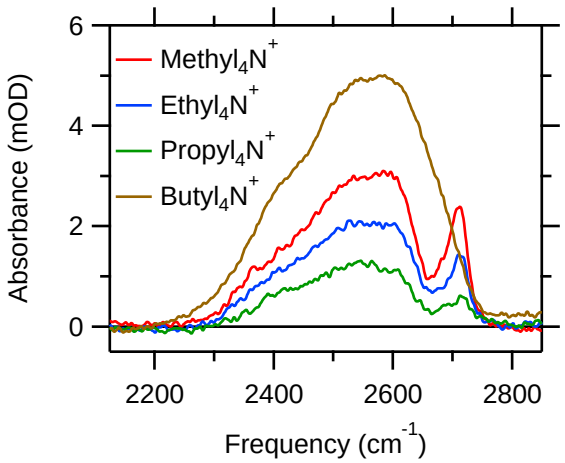

Fig. S 14: Unnormalized O−D stretch spectra recorded at a potential of −1.02 V in the presence of the different cations as indicated.

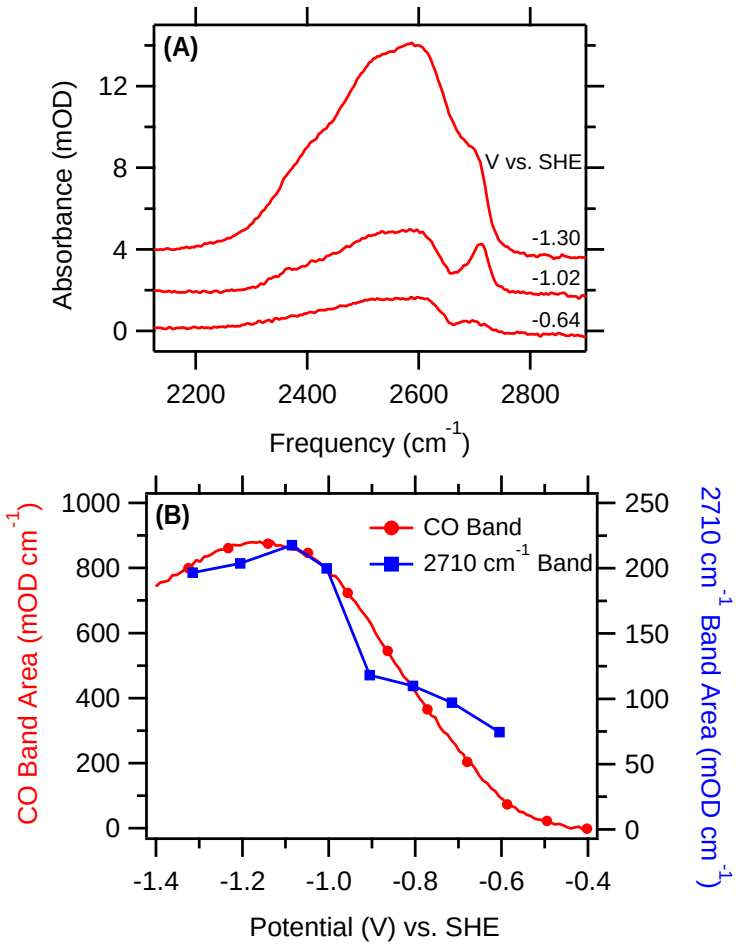

Fig. S 15: (A) Representative O−D stretch spectra in 0.1 M methyl$_4$N$^+$ chloride in D_2O. (B) Integrated band areas of the C≡O stretch band (red circles) and O−D stretch band at 2710 cm^{-1} (blue squares) as a function of applied potential.

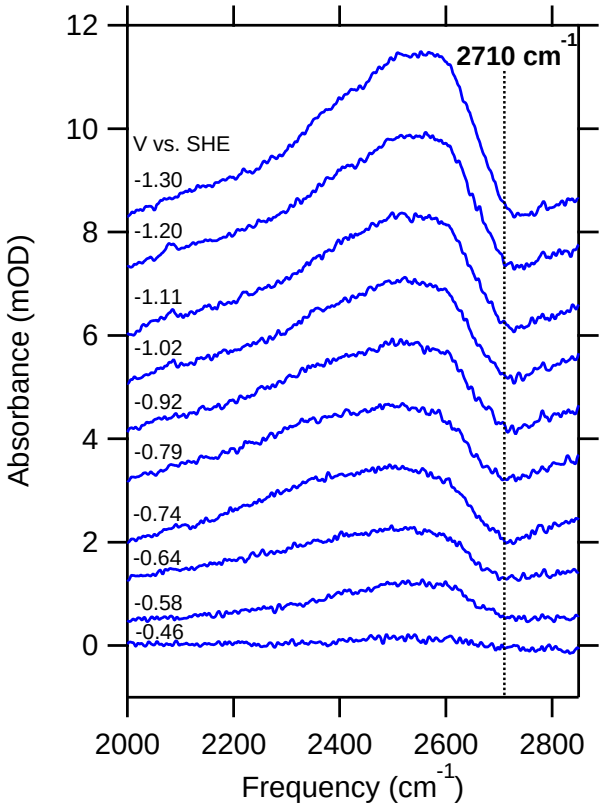

Fig. S 16: O−D stretch spectra in Ar-purged 0.1 M methyl$_4$N$^+$ chloride electrolyte confirm that the 2710 cm^{-1} band is only present for the CO-covered Cu electrode (Figure 6 of the main text).

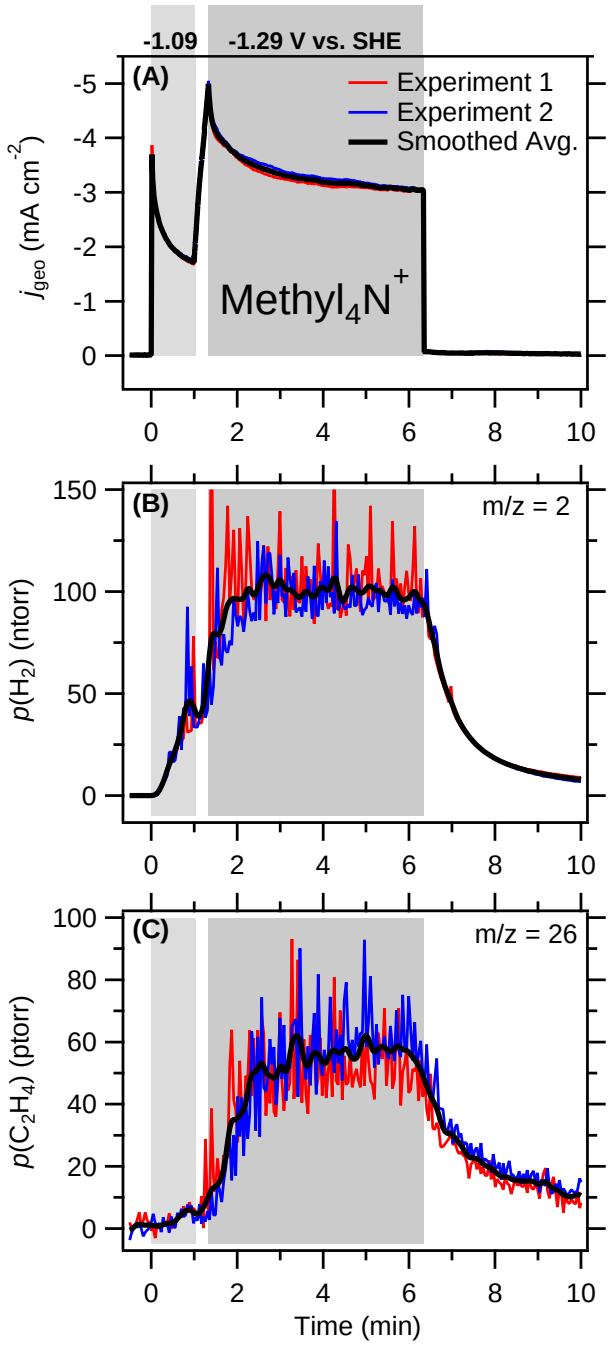

Fig. S 17: Raw DEMS data for methyl$_4$N$^+$. (A) Electrochemical current density, (B) H_2 partial pressure, and (C) C_2H_4 partial pressure recorded during two independent experiments (thin red and blue traces) of CO electroreduction on Cu. The thick black trace represents the smoothed average of the two experiments.

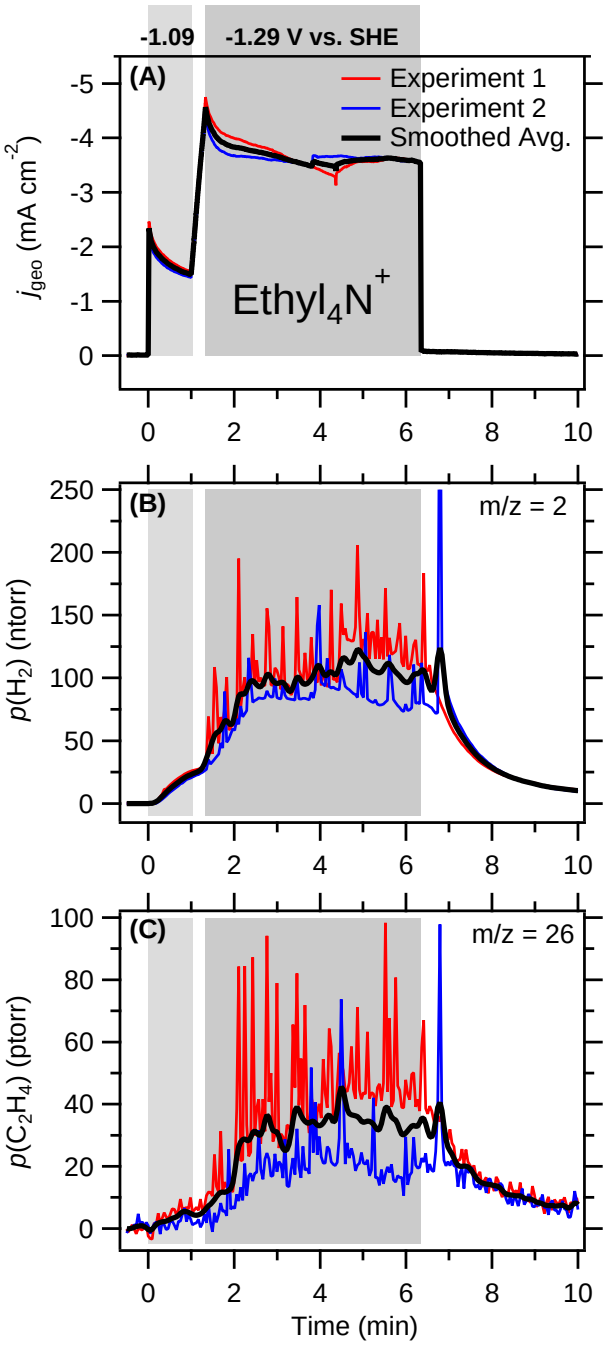

Fig. S 18: Raw DEMS data for ethyl$_4$N$^+$. (A) Electrochemical current density, (B) H_2 partial pressure, and (C) C_2H_4 partial pressure recorded during two independent experiments (thin red and blue traces) of CO electroreduction on Cu. The thick black trace represents the smoothed average of the two experiments.

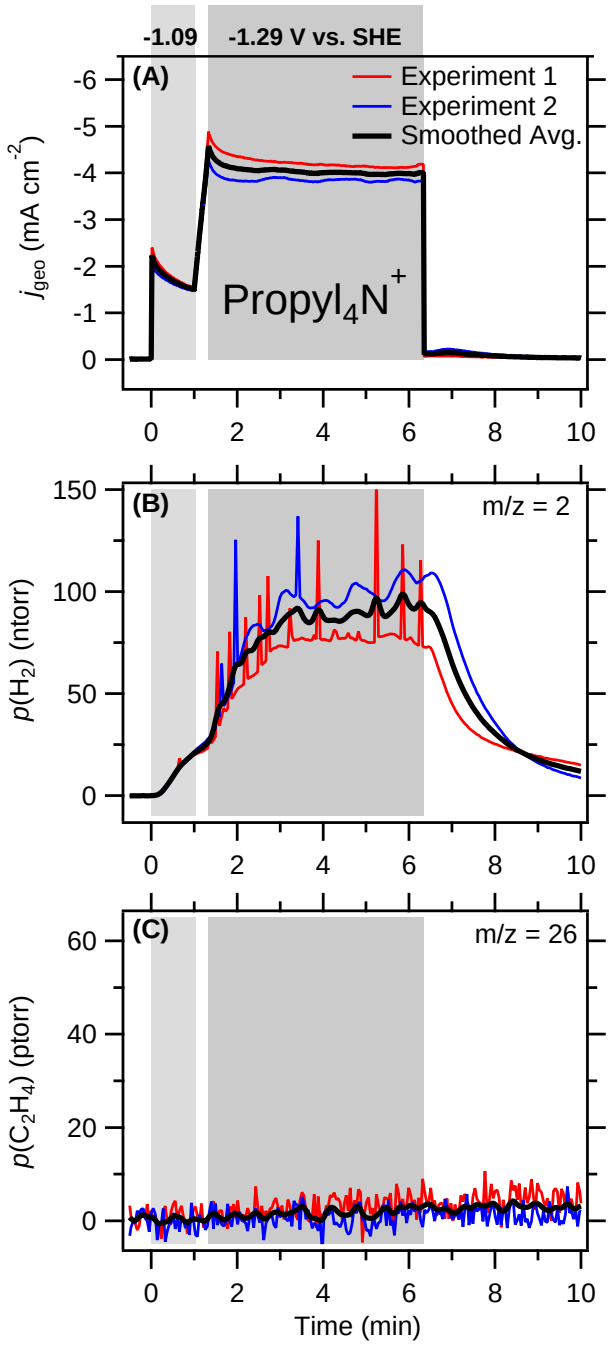

Fig. S 19: Raw DEMS data for propyl$_4$N$^+$. (A) Electrochemical current density, (B) H_2 partial pressure, and (C) C_2H_4 partial pressure recorded during two independent experiments (thin red and blue traces) of CO electroreduction on Cu. The thick black trace represents the smoothed average of the two experiments.

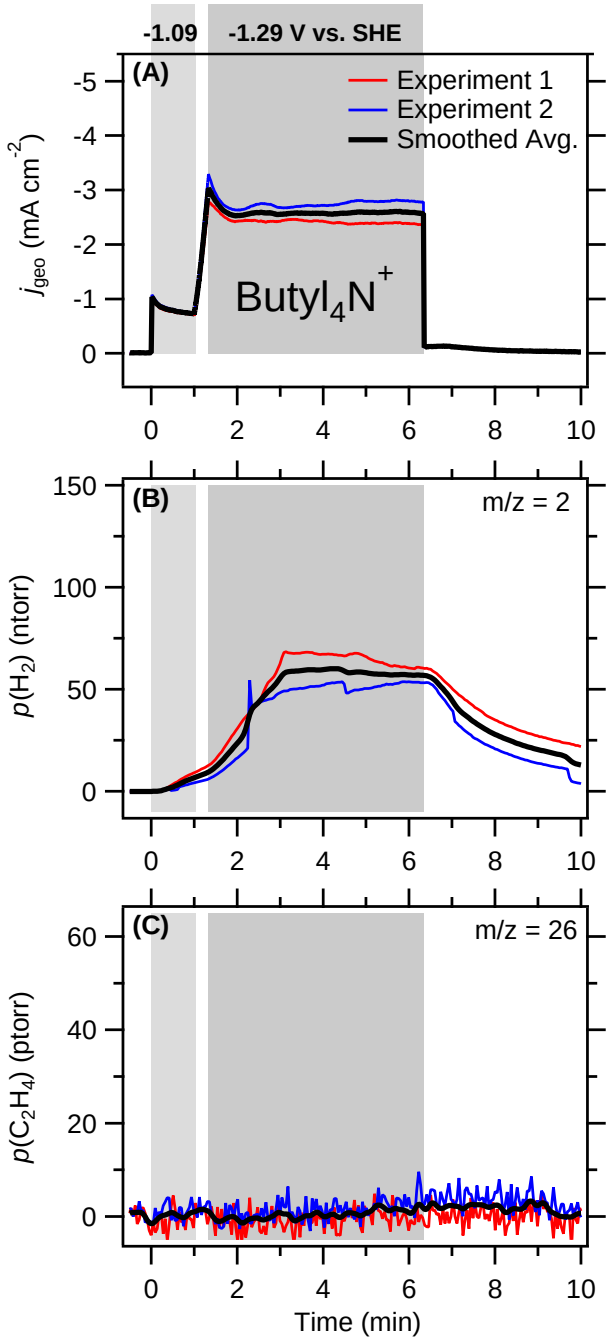

Fig. S 20: Raw DEMS data for butyl$_4$N$^+$. (A) Electrochemical current density, (B) H_2 partial pressure, and (C) C_2H_4 partial pressure recorded during two independent experiments (thin red and blue traces) of CO electroreduction on Cu. The thick black trace represents the smoothed average of the two experiments.

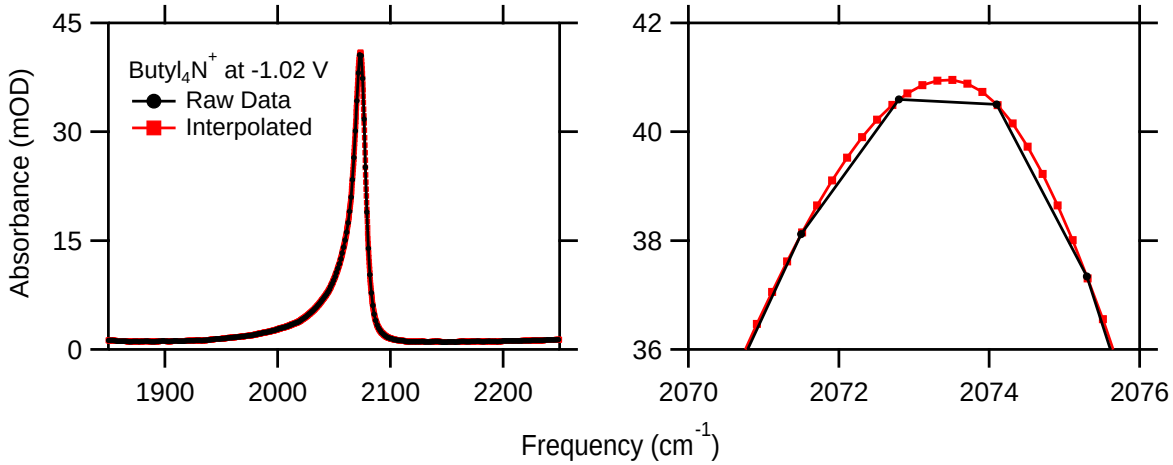

Fig. S 21: An example of FTIR data interpolation. The data presented was collected in the presence of 0.1 M butyl$_4$N$^+$ in D_2O at potential of -1.02 V. The interpolated data (red) captures the CO peak frequency more accurately than the raw data (black).

References

(1) Wallace, W. E. *Mass Spectra in NIST Chemistry WebBook, NIST Standard Reference Database Number 69, Eds. P.J. Linstrom and W.G. Mallard*; National Institute of Standards and Technology: Gaithersburg MD, 20899, 2019.

(2) Waszczuk, P.; Zelenay, P.; Sobkowski, J. Surface Interaction of Benzoic Acid with a Copper Electrode. *Electrochim. Acta* **1995**, *40*, 1717–1721.